JCB Article

Induction of maturation-promoting factor during *Xenopus* oocyte maturation uncouples Ca^{2+} store depletion from store-operated Ca^{2+} entry

Khaled Machaca and Shirley Haun

Department of Physiology and Biophysics, University of Arkansas Medical Science, Little Rock, AR 72205

During oocyte maturation, eggs acquire the ability to generate specialized Ca^{2+} signals in response to sperm entry. Such Ca^{2+} signals are crucial for egg activation and the initiation of embryonic development. We examined the regulation during *Xenopus* oocyte maturation of store-operated Ca^{2+} entry (SOCE), an important Ca^{2+} influx pathway in oocytes and other nonexcitable cells. We have previously shown that SOCE inactivates during *Xenopus* oocyte meiosis. SOCE inactivation may be important in preventing premature egg activation. In this study, we investigated the correlation between SOCE inactivation and the Mos–mitogen-activated protein kinase (MAPK)–maturation-promoting factor (MPF) kinase cascade, which drives *Xenopus* oocyte maturation. SOCE inactivation at germinal vesicle breakdown coincides with an increase in the levels of MAPK and MPF. By differentially inducing Mos, MAPK, and MPF, we demonstrate that the activation of MPF is necessary for SOCE inactivation during oocyte maturation. In contrast, sustained high levels of Mos kinase and the MAPK cascade have no effect on SOCE activation. We further show that preactivated SOCE is not inactivated by MPF, suggesting that MPF does not block Ca^{2+} influx through SOCE channels, but rather inhibits coupling between store depletion and SOCE activation.

Introduction

Sexual reproduction requires germ cell fusion, and correct execution of the developmental program. In many species, including mammals and amphibians, fully-grown oocytes in the ovary are not able to be fertilized or support embryonic development, unless they undergo oocyte maturation. Oocyte maturation corresponds to a complex differentiation program that transforms the oocyte into an egg that is fertilization competent, and capable of supporting early embryonic development (Yamashita et al., 2000).

The amphibian oocyte represents one of the best-characterized models for oocyte maturation, at a biochemical as well as morphological level (Bement and Capco, 1990). In *Xenopus laevis*, fully grown oocytes (stage VI) in the ovary are arrested at prophase of meiosis I. During oocyte maturation, cells enter meiosis, undergo germinal vesicle (nuclear envelope) breakdown (GVBD),* complete meiosis I with the extrusion of a polar body, and arrest at metaphase of the second meiotic division (MII) until fertilization (Masui and Clarke, 1979). We will refer to mature cells arrested at MII as eggs, to differentiate them from immature oocytes arrested at prophase I. *Xenopus* oocyte maturation is initiated in response to the hormone progesterone, which induces a signal transduction cascade culminating in the activation of maturation-promoting factor (MPF) (for recent review see Nebreda and Ferby, 2000). MPF is a complex, composed of a serine/threonine kinase ($p34^{cdc2}$) subunit and a regulatory cyclin B subunit. MPF activation is necessary and sufficient for GVBD and entry into meiosis (Smith, 1989). Progesterone-induced maturation requires translation of Mos kinase, which induces the MAP kinase cascade, resulting in MPF activation (Sagata, 1997). In addition to the Mos–mitogen-activated protein kinase (MAPK) cascade, other signaling cascades are activated in parallel, resulting in rapid MPF induction. The polo-like kinase cascade is thought to activate Cdc25C phosphatase, which dephosphorylates and activates MPF (Qian et al., 1999, 2001).

Address correspondence to Khaled Machaca, Ph.D., Department of Physiology, Slot 505, 4301 West Markham St., University of Arkansas Medical Science, Little Rock, AR 72205. Tel.: (501) 603-1596. Fax: (501) 686-8167. E-mail: machacakhaleda@uams.edu

*Abbreviations used in this paper: BAPTA, 1,2-bis(2-aminophenoxy) ethane-*N*,*N*,*N*′,*N*′-tetraacetic acid; CSF, cytostatic factor; GST, glutathione-*S*-transferase; GVBD, germinal vesicle breakdown; $GVBD_i$, time of initial appearance of GVBD; $GVBD_{50}$, time at which 50% of the oocyte undergo GVBD; I_{SOCE}, SOCE current; I–V, current–voltage; MAPK, mitogen-activated protein kinase; MEK, mitogen-activated protein kinase kinase; MII, second meiotic division; MPF, maturation-promoting factor; P-MAPK, phospho-MAPK; SOCE, store-operated Ca^{2+} entry.

Key words: calcium signaling; store-operated Ca^{2+} entry; oocyte maturation; *Xenopus laevis*; maturation-promoting factor

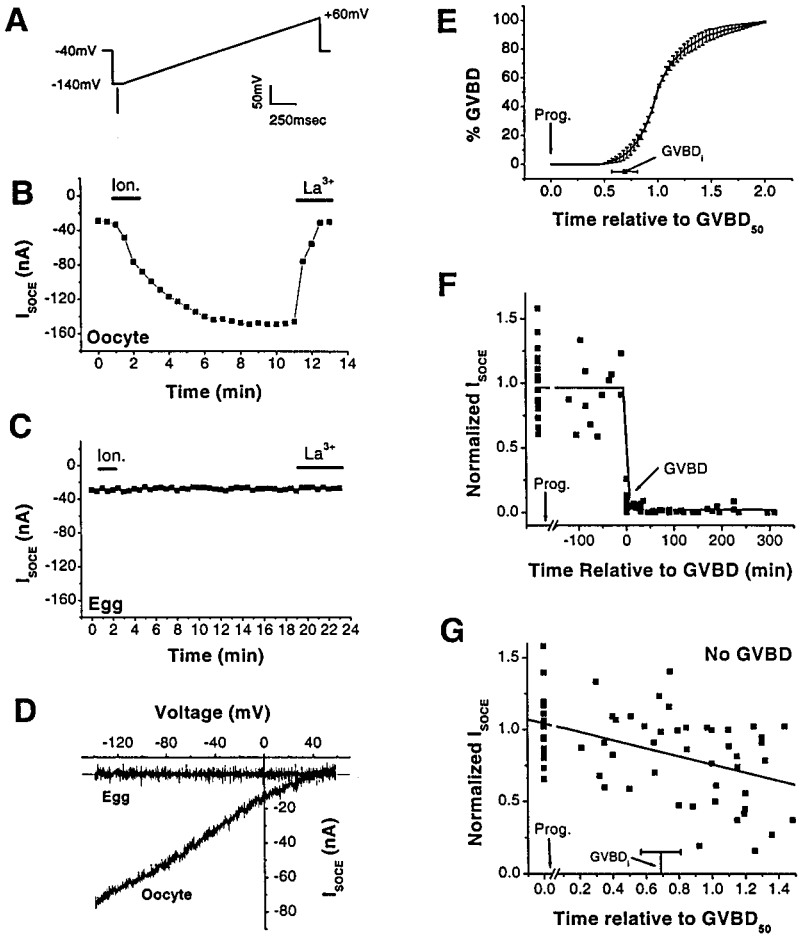

Figure 1. **I_{SOCE} during *Xenopus* oocyte maturation.** (A) Voltage protocol used to measure I_{SOCE} development and I–V relationship. The membrane potential was stepped to −140 mV (100 ms), and then ramped from −140 to +60 mV (2 s) from a −40 mV holding potential. The protocol was applied once every 30 s. (B and C) I_{SOCE} development after Ca^{2+} store depletion with ionomycin (10 μM) in an oocyte (B) and an egg (C). Cells were injected with 7 nmol BAPTA to allow for I_{SOCE} recording (Machaca and Haun, 2000). The current at −140 mV (A, arrow) was plotted over time. La^{3+} (100 μM) was added at the end of the experiment to block SOCE and obtain a measure of absolute I_{SOCE}. (D) Representative I–V relationships obtained from the ramp voltage stimulation shown in A from an oocyte and an egg. I–V relationships were obtained by subtracting the current after La^{3+} addition from the current before addition. (E) Time course of progesterone-mediated GVBD. Progesterone was added to a population of at least 50 oocytes, and the occurrence of GVBD over time was recorded by following white spot appearance on the animal pole. The data shown represent the average ± SE from seven donor females. The time of $GVBD_i$ ± SD is also shown. $GVBD_i$ represents the time at which GVBD was first observed in the population. (F and G) I_{SOCE} levels from individual oocytes at different times during oocyte maturation. Each square represents the current from a single cell. I_{SOCE} data from oocytes are shown before progesterone addition. The data was normalized to average current in oocytes. I_{SOCE} data from 80 cells at different times during maturation are shown in F. (G) I_{SOCE} levels from cells incubated in progesterone without undergoing GVBD ($n = 63$). The average time ± SD of $GVBD_i$ is shown for reference.

An important component of oocyte maturation is differentiation of the Ca^{2+} signaling machinery, which is essential for egg activation after fertilization. An increase in cytoplasmic Ca^{2+} at fertilization is the universal signal to initiate development in all species investigated (Homa et al., 1993; Stricker, 2000). Ca^{2+} signals generated at fertilization in *Xenopus* have specific spatial and temporal features that are presumably important for successful egg activation. For example, Ca^{2+} signals are crucial for the block to polyspermy (Cross, 1981; Kline and Nuccitelli, 1985), through the induction of membrane depolarization (Machaca et al., 2001) and the activation of cortical granule fusion (Wolf, 1974; Grey et al., 1976). Increased Ca^{2+} is also responsible for releasing the MII block by inactivating cytostatic factor (CSF) (Meyerhof and Masui, 1979). Therefore, during oocyte maturation, Ca^{2+} signaling pathways undergo their own differentiation followed by functionally significant consequences. In this study, we investigate the regulation of store-operated Ca^{2+} entry (SOCE) during *Xenopus* oocyte maturation. SOCE is a ubiquitous Ca^{2+} entry pathway in nonexcitable cells, activated in response to depletion of intracellular Ca^{2+} stores (Parekh and Penner, 1997). SOCE is important for a variety of physiological functions, including regulation of exocytosis (Koizumi and Inoue, 1998; Fomina and Nowycky, 1999), modulation of Ca^{2+} waves (Girard and Clapham, 1993; Dolmetsch and Lewis, 1994), and activation of T lymphocytes (Fanger et al., 1995; Serafini et al., 1995). The mechanism by which Ca^{2+} store depletion activates SOCE is controversial. Three primary models have been proposed with experimental evidence for each: direct physical coupling between SOCE channels and a Ca^{2+} sensor (Berridge, 1995; Kiselyov et al., 1998); activation of SOCE channels by a diffusible messenger (Randriamampita and Tsien, 1993; Csutora et al., 1999); and exocytotic insertion of SOCE channels in the plasma membrane (Somasundaram et al., 1995; Yao et al., 1999).

We have previously demonstrated that SOCE inactivates during *Xenopus* oocyte maturation (Machaca and Haun, 2000), and were interested in elucidating the mechanisms mediating this inactivation. In this study, we show that the induction of MPF is necessary for SOCE inactivation. In contrast, the activation of kinase cascades upstream of MPF does not affect SOCE. However, MPF does not appear to inhibit Ca^{2+} influx through SOCE channels, rather it blocks the coupling mechanism between store depletion and SOCE activation.

Results

Levels of SOCE during progesterone-induced oocyte maturation

Depletion of intracellular Ca^{2+} stores activates SOCE in stage VI *Xenopus* oocytes (Fig. 1 B). The SOCE current (I_{SOCE}) was measured as previously described (Machaca and Haun, 2000), using a ramp voltage stimulation from

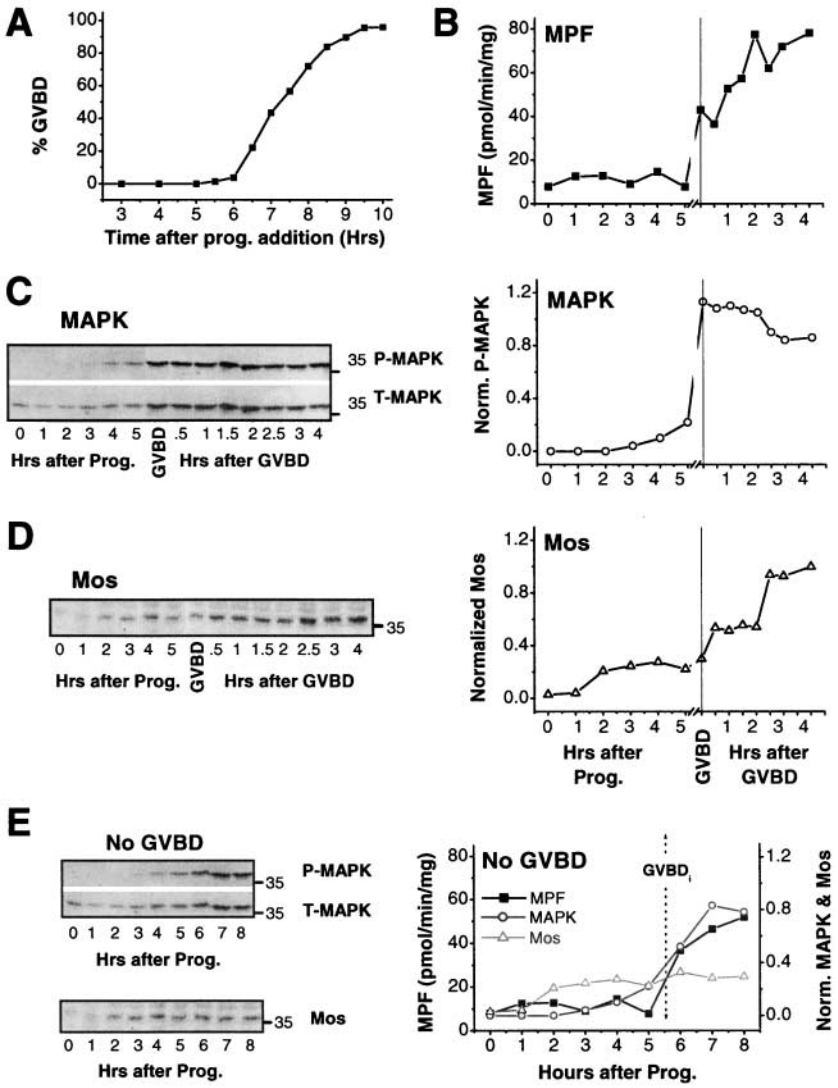

Figure 2. **Time course of MPF, MAPK, and Mos activation during progesterone-induced maturation.** (A) Time course of GVBD. $GVBD_i$ occurred at 5.5 h, and $GVBD_{50}$ ~7.25 h after progesterone addition. At each time point, five cells were pooled to quantify kinase activity. (B–D) MPF, P-MAPK, and Mos levels during oocyte maturation. MPF activity was measured as the histone H1 kinase activity as described in Materials and methods. The levels of P-MAPK and Mos were determined by Western blot analysis using a P-MAPK–specific and anti-Mos antibody, respectively, as described in Materials and methods. In the case of MAPK, the same blot was reprobed with an antibody that detects total MAPK (T-MAPK) levels, showing that MAPK was present in the lysates but was not phosphorylated. To be able to compare P-MAPK and Mos levels between different experiments, we always ran a positive control lysate from eggs on every gel, and normalized P-MAPK and Mos levels to that sample. Therefore, Western data for P-MAPK and Mos throughout this manuscript are normalized to the same egg lysate (see Materials and methods for more details). The time scale is divided into two phases: after progesterone addition; and after GVBD. The 35-kD molecular mass marker is shown on the right of the gels. (E) MPF, P-MAPK, and Mos levels in cells treated with progesterone, but that did not undergo GVBD. $GVBD_i$ is indicated for reference. This time course of kinase activation is representative of five similar experiments.

−140mV to +60mV (Fig. 1 A). Current at −140mV (Fig. 1 A, arrow) is plotted over time to visualize the activation of I_{SOCE} after Ca^{2+} store depletion (Fig. 1 B). Depletion of intracellular Ca^{2+} stores in eggs induced to mature with progesterone, did not activate SOCE (Fig. 1 C). A representative current–voltage (I–V) relationship from an oocyte reveals the typical inward rectifying I–V relationship that is a signature of I_{SOCE} (Fig. 1 D). In contrast, the I–V relationship in an egg is flat, indicating that store depletion does not activate SOCE in mature eggs (Fig. 1 D).

The time course of oocyte maturation varies between different females. When comparing data from different donors it is helpful to normalize to the time at which 50% of the oocyte population undergo GVBD ($GVBD_{50}$) (Fig. 1 E). GVBD is scored based on the appearance of a white spot on the animal pole due to pigment dispersal (Smith, 1989). In these experiments (Fig. 1, E–G), $GVBD_{50}$ was reached 5.6 ± 0.4 h after progesterone addition ($n = 7$). The initial appearance of GVBD in the population ($GVBD_i$) was reached 3.8 ± 0.2 h after progesterone addition ($n = 7$) (Fig. 1 E). We measured I_{SOCE} at different time points during the maturation process (Fig. 1, F and G). Before GVBD, there was no significant change in I_{SOCE} levels in maturing cells as compared with untreated oocytes (Fig. 1 F). However, I_{SOCE} abruptly inactivated as soon as GVBD was observed, and remained inactivated for the remainder of the maturation process (Fig. 1 F). Therefore, once maturing oocytes reach the GVBD stage, and for the rest of the maturation period, SOCE can no longer be activated by store depletion. We have previously shown that this acute inactivation of SOCE does not correlate with the gradual decrease in membrane surface area observed during oocyte maturation. Nor is it due to cortical granule fusion upon Ca^{2+} store depletion, which releases proteases at the cell surface (Machaca and Haun, 2000).

We also examined I_{SOCE} levels in oocytes incubated in progesterone for prolonged periods of time, without undergoing GVBD (GVBD negative) (Fig. 1 G). In the majority of such cells (34/44), I_{SOCE} was detected at levels similar to those in control oocytes (Fig. 1 G), indicating a correlation between I_{SOCE} inactivation and GVBD. However, there was a trend for decreased levels of I_{SOCE} at time points longer than 0.8 $GVBD_{50}$ (Fig. 1 G). GVBD is followed by white spot appearance, indicating completion of nuclear envelope breakdown. Nonetheless, GVBD initiates before white spot appearance as the nuclear envelope breaks down gradually, in a

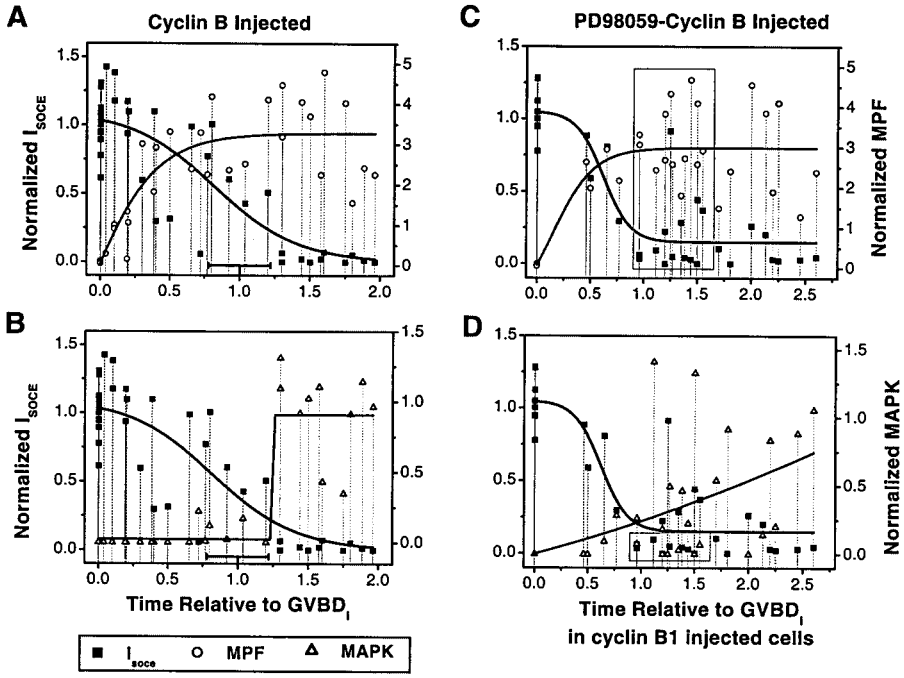

Figure 3. **Correlation between I_{SOCE} and MPF and P-MAPK levels after Δ87cyclin B1 protein injection.** Oocytes were either directly injected with Δ87cyclin B1 protein (A and B) or preincubated in the MEK inhibitor PD98059 (50–100 μM) for 0.5–2 h before Δ87cyclin B1 injection. I_{SOCE} levels were recorded at various times after Δ87cyclin B1 injection. After I_{SOCE} recording, individual cells were lysed and assayed for MPF and P-MAPK levels. This allowed us to obtain I_{SOCE} (squares), MPF (circles), and P-MAPK (triangles) levels from the same oocyte. The data for individual cells are connected by drop lines to help in matching I_{SOCE} and kinase activity from the same cell. For Δ87cyclin B1 and PD98059-Δ87cyclin B1 injections, current and kinase data from 40 and 33 cells, respectively, are shown. I_{SOCE} levels were normalized to the levels in untreated oocytes, and MPF and MAPK levels were normalized to the levels found in fully mature eggs, as described in Fig. 2. The time scale was normalized to the time at which GVBD initially appeared in the population ($GVBD_i$) after Δ87cyclin B1 injection. The standard deviation of $GVBD_i$ is shown in A and B ($n = 7$). PD98059-treated cells are plotted on a time scale normalized to $GVBD_i$ in Δ87cyclin B1–injected cells (A and B). Individual cell data were fitted with a Boltzman function to obtain a general trend of I_{SOCE} inactivation and the activation of the different kinases.

polarized fashion beginning at the vegetal face of the nucleus (Colman et al., 1985). Therefore, cells in which I_{SOCE} activity was decreased could have initiated GVBD, consistent with a temporal correlation between GVBD and I_{SOCE} inactivation.

I_{SOCE} inactivation could be a direct downstream consequence of GVBD. To test this possibility, we removed the nucleus from oocytes (enucleated), and matured them in progesterone. We recorded I_{SOCE} from enucleated cells when 100% of the control oocyte group underwent GVBD. Under these conditions in both control and enucleated cells, I_{SOCE} was completely inactivated (unpublished data). Furthermore, enucleated cells incubated for the same time in the absence of progesterone had I_{SOCE} levels similar to those of untreated oocytes, indicating that removal of the nucleus did not lead to I_{SOCE} inactivation. Thus, physical breakdown of the nuclear envelope is not a prerequisite for I_{SOCE} inactivation.

Time course of Mos, MAPK, and MPF activation during oocyte maturation

As discussed above, oocyte maturation is driven by kinase cascades that lead to MPF activation and entry into meiosis. We next examined whether these kinases are involved in I_{SOCE} inactivation. We focused our attention on the Mos–MAPK signal transduction cascade, which is the primary pathway for MPF activation in *Xenopus* oocytes (Palmer and Nebreda, 2000). Fig. 2 summarizes the time course of Mos, MAPK, and MPF activation during progesterone-induced oocyte maturation. In this experiment, $GVBD_i$ occurred at 5.5 h, and $GVBD_{50}$ was reached ~7 h after progesterone addition (Fig. 2 A). MPF activity increased at $GVBD_i$ and then decreased slightly 30 min after GVBD, indicative of the transition between meiosis I and II. This was followed by a plateau phase of high MPF activity for the reminder of maturation (Fig. 2 B). MAPK activation could be followed with a specific antibody that recognized the phosphorylated (activated) form of the kinase (Fig. 2 C). Phospho-MAPK (P-MAPK) was first detected 3 h after progesterone addition, and increased slowly with a jump at GVBD (Fig. 2 C). Mos kinase levels rose to a low level plateau 2 h after progesterone addition (Fig. 2 D), before any increase in P-MAPK was observed. This is consistent with Mos's role as the upstream kinase that activates the MAPK cascade (Sagata, 1997). Mos protein levels remained at the low plateau level until 30 min after GVBD, when a significant increase was observed (Fig. 2 D). This is presumably due to the activation of MPF, which stabilizes the Mos protein (Sagata, 1997). As shown in Fig. 1, SOCE inactivated at the GVBD stage of meiosis, at the same time that MPF and P-MAPK levels increased (Fig. 2, B and C). It is therefore possible that either MPF, MAPK, or both are involved in SOCE inactivation.

We have also determined the time course of activation of these kinases in cells treated with progesterone but that have not undergone GVBD (Fig. 2 E). In this population, MPF activity started to increase past the $GVBD_i$ time point, eventually reaching levels similar to those observed in GVBD positive cells (Fig. 2 E). P-MAPK levels also increased gradually after $GVBD_i$, whereas Mos protein remained at the preGVBD plateau level (Fig. 2 E). Increased MPF and MAPK activity in GVBD negative cells, is consistent with one or both kinases being involved in SOCE inactivation. This is because SOCE levels are lower in oocytes at this stage of maturation (Fig. 1 G).

SOCE inactivates independently of the MAPK cascade

The time course of I_{SOCE} inhibition and kinase activation during progesterone-induced maturation (Figs. 1 and 2),

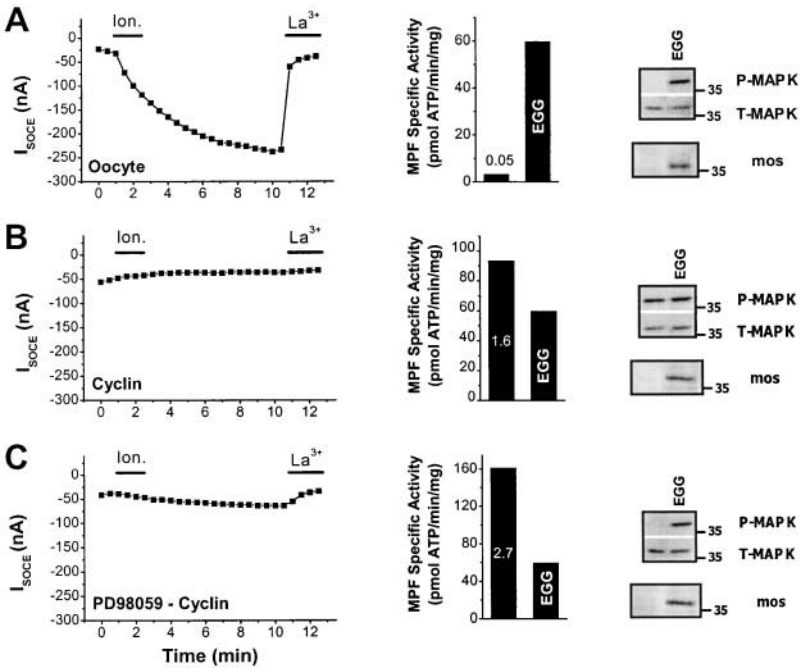

Figure 4. **Representative individual cell data from Δ87cyclin B1–injected cells.** MPF, P-MAPK, and Mos Western data are shown in conjunction with the levels of each kinase in fully mature eggs (EGG). (A) I_{SOCE} was activated in response to store depletion with ionomycin (10 μM) in an oocyte, and MPF, P-MAPK, and Mos were not detected. (B) A representative oocyte injected with Δ87cyclin B1. I_{SOCE} was not activated in response to store depletion. MPF and P-MAPK levels were 1.6 and 0.9 times those in eggs, whereas Mos kinase was not detected in this oocyte. (C) A representative oocyte preincubated with PD98059 (100 μM) before Δ87cyclin B1 injection. I_{SOCE} was not activated in response to store depletion, MPF levels were 2.7 times higher than those found in the control egg lysate, and both P-MAPK and Mos were not detectable.

suggest that the MAPK cascade and/or MPF could be involved in SOCE inactivation. To directly test this possibility we manipulated the levels of MAPK and MPF, and determined the effect on SOCE. This was accomplished by injecting cyclin B1 protein in the presence or absence of a mitogen-activated protein kinase kinase (MEK) inhibitor (Fig. 3). MEK is the upstream kinase that phosphorylates and activates MAPK (Palmer and Nebreda, 2000). Cyclin B1 binds and activates $p34^{cdc2}$, the catalytic subunit of MPF, thus rapidly increasing MPF activity. Cyclin B1 injections have been shown to induce GVBD in the absence of progesterone (Freeman et al., 1991).

In these experiments we wanted to correlate the levels of kinase activity with I_{SOCE}. However, the asynchronous nature of *Xenopus* oocyte maturation introduced significant variability, making such correlations difficult to draw. To circumvent this problem, we performed these studies on single oocytes, i.e., we recorded I_{SOCE} levels and MPF and MAPK activity from individual cells. This allowed us to directly correlate the activity of these kinases with I_{SOCE} levels in the same oocyte. The data is plotted over a time scale normalized to $GVBD_i$, to determine whether there is a correlation between I_{SOCE} inactivation and GVBD. Injection of cyclin B1 protein into oocytes induced GVBD with an average time of 2 ± 0.4 h ($n = 7$ donor females). As is the case after progesterone treatment, I_{SOCE} was completely inactivated in cells that had undergone GVBD in response to cyclin B1 injection. However, the kinetics of MPF and I_{SOCE} inactivation were more complex (Fig. 3 A). Shortly after cyclin B1 injection, MPF activity increased to levels similar to those observed in eggs, and eventually plateaued at MPF levels two- to fourfold those in eggs (Fig. 3 A). The time course of I_{SOCE} inactivation lagged behind that of MPF activity (Fig. 3 A). P-MAPK levels increased significantly only after $GVBD_i$, when I_{SOCE} was completely inactivated (Fig. 3 B). I_{SOCE} began to inactivate before P-MAPK became detectable (Fig. 3 B), but complete inactivation of I_{SOCE} correlated with increased P-MAPK levels.

The time delay between MPF activation and I_{SOCE} inactivation was also evident for GVBD, which is a known target of MPF (Bement and Capco, 1990). Therefore, ectopic activation of MPF by cyclin B1 injection did not faithfully reproduce the downstream effects of progesterone-induced MPF activation. In the case of progesterone, an increase in MPF levels coincided with GVBD (Fig. 2 B). The reason for the lag period between MPF activation by cyclin B1 and GVBD is not clear to us. We suggest that it could be due to mislocalization of MPF after cyclin B1 injection, thus delaying MPF action on downstream targets.

To directly test whether MAPK activation is required for I_{SOCE} inactivation we treated cells with the MEK inhibitor PD98059, which blocks MAPK activation. This allowed us to obtain a population of cells containing high MPF activity, without activating the MAPK cascade (Fig. 3, C and D). Injection of cyclin B1 into PD98059-treated oocytes induced the activation of MPF (Fig. 3 C) with a similar time course and to comparable levels as control oocytes (Fig. 3 A). In this case there also was a strong temporal correlation between GVBD and I_{SOCE} inactivation. Pretreating oocytes with PD98059 delayed but did not completely block MAPK activation, as some cells at later time points showed high levels of P-MAPK (Fig. 3 D). However, we could easily define a population of cells, between 0.9 and 1.6 $GVBD_i$, in which MAPK activity was completely blocked by PD98059 (Fig. 3 D, box). All of these cells had high levels of MPF activity (one- to fourfold that in eggs) (Fig. 3 C, box). Such cells with high MPF activity and no detectable P-MAPK had completely inactivated I_{SOCE} (Fig. 3, C and D). This indicates that activation of the MAPK cascade is not required for I_{SOCE} inactivation.

Fig. 4 shows examples of single cells illustrating the need for MPF, but not MAPK, activation for I_{SOCE} inactivation. In a

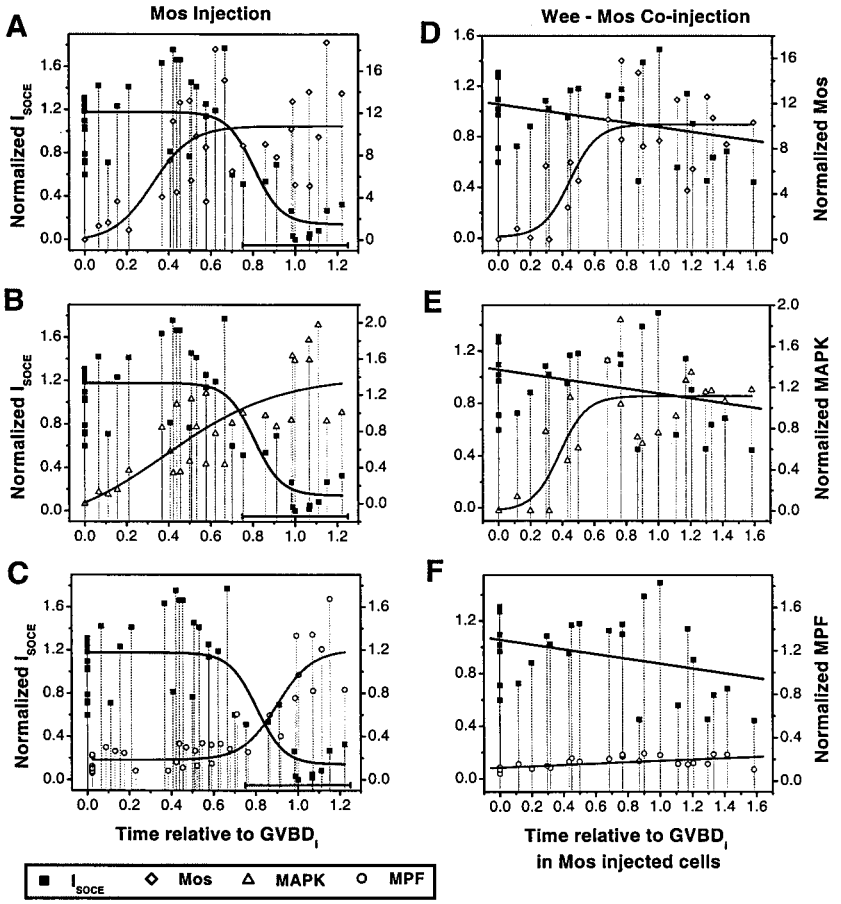

Figure 5. **Correlation between I_{SOCE} and Mos, P-MAPK, and MPF levels after injection of GST–Mos RNA.** GST–Mos is a fusion protein between GST and *Xenopus* Mos, which allowed the separation between endogenous Mos (39 kD) and recombinant, injected GST–Mos (64 kD) (see Materials and methods). Oocytes were either directly injected with 10 ng GST–Mos RNA (A–C) or preinjected with 10 ng of GST–107Wee1 (Wee) 13–16 h before Mos RNA injection. GST–107Wee1 is a constitutively active form of the Wee1 kinase, which blocks MPF activation (Howard et al., 1999). I_{SOCE} levels recorded at various times after GST–Mos RNA injection. After I_{SOCE} recording, individual cells were lysed and assayed for kinase activities. This allowed us to obtain I_{SOCE} (squares), Mos (diamonds), P-MAPK (triangles), and MPF (circles) levels from the same oocyte. For Mos and Wee1–Mos injections, current and kinase data from 40 and 27 cells, respectively, are shown. The plotted Mos data is for GST–Mos protein levels, as endogenous Mos was not detected in these experiments. The data for individual cells are connected by drop lines to help in matching I_{SOCE} and kinase activity from the same cell. I_{SOCE} levels were normalized to the levels in untreated oocytes, and Mos, MAPK, and MPF levels were normalized to the levels found in fully mature eggs as described in Fig. 2 and Materials and methods. The time scale was normalized to $GVBD_i$, the standard deviation of which is shown in A–C ($n = 5$). Cells preinjected with GST–107Wee1 were plotted on the same time scale as GST–Mos-injected cells (D–F). Individual cell data were fitted with a Boltzman function to obtain a general trend of I_{SOCE} inactivation and the activation of the different kinases.

control untreated oocyte MPF, MAPK, and Mos activities were undetectable, and I_{SOCE} was activated in response to store depletion (Fig. 4 A). In contrast, no I_{SOCE} could be detected after store depletion in a cyclin B1–injected cell (Fig. 4 B). In this case, cyclin B1 injection induced MPF and P-MAPK activation (1.6- and 0.9-fold egg levels, respectively), but little Mos protein was detected (Fig. 4 B). This argues that Mos kinase is not required for SOCE inactivation.

Fig. 4 C shows I_{SOCE} and kinase data from an oocyte treated with the MEK inhibitor PD98059 before cyclin B1 injection. This resulted in robust activation of MPF (2.7-fold egg level), without activating either MAPK or inducing Mos protein accumulation (Fig. 4 C). In this cell, I_{SOCE} was almost completely inactivated, showing that SOCE inactivation can occur independently of the MAPK cascade and Mos.

MPF activation is necessary for I_{SOCE} inactivation

We next examined whether MPF activation is required for SOCE inactivation. We initiated oocyte maturation by injecting Mos RNA into oocytes in the presence or absence of a specific MPF inhibitor, the Wee1 kinase (Mueller et al., 1995) (Fig. 5). These experiments also allowed us to test whether prolonged activation of Mos and the MAPK cascade can induce I_{SOCE} inactivation. Mos kinase is necessary and sufficient for oocyte maturation (Sagata, 1997).

To determine the correlation between I_{SOCE} inactivation and levels of Mos, MAPK, and MPF, we recorded I_{SOCE} and measured the levels of the three aforementioned kinases in individual cells (Fig. 5). The data was plotted on a time scale normalized to $GVBD_i$, which occurred 5.8 ± 1.4 h after Mos RNA injection ($n = 5$ donor females). Soon after the injection of Mos RNA (0.1 $GVBD_i$), Mos levels were similar to those observed in eggs. Mos protein levels increased gradually over time, reaching a plateau at ~10-fold egg levels (Fig. 5 A). Note that we measured recombinant glutathione-*S*-transferase (GST)–Mos levels in these experiments, and did not detect endogenous Mos protein expression (see Fig. 6). I_{SOCE} did inactivate in response to Mos RNA injection (Fig. 5 A). The time course of I_{SOCE} inactivation was significantly delayed compared with Mos activation. Mos protein levels reached egg levels at 0.1 $GVBD_i$, whereas I_{SOCE} began to inactivate around 1 $GVBD_i$ (Fig. 5 A). This time lag translates to ~5.2 h of high Mos activity before I_{SOCE} inactivated. In this case we know that ectopic expression of GST–Mos was effectively targeting at least one of its downstream effectors, the MAPK cascade. This is because P-MAPK increased with a similar time course to Mos (Fig. 5 B), reaching a plateau at ~1.3-fold egg levels. This suggests that Mos kinase is not directly involved in I_{SOCE} inactivation. We have shown above that activation of the MAPK cascade is not required for I_{SOCE} inactivation. The lack of correlation between P-MAPK and I_{SOCE} levels after Mos injection supports this conclusion.

We have also measured MPF levels from the same cells (Fig. 5 C). In this case I_{SOCE} inactivation followed the same

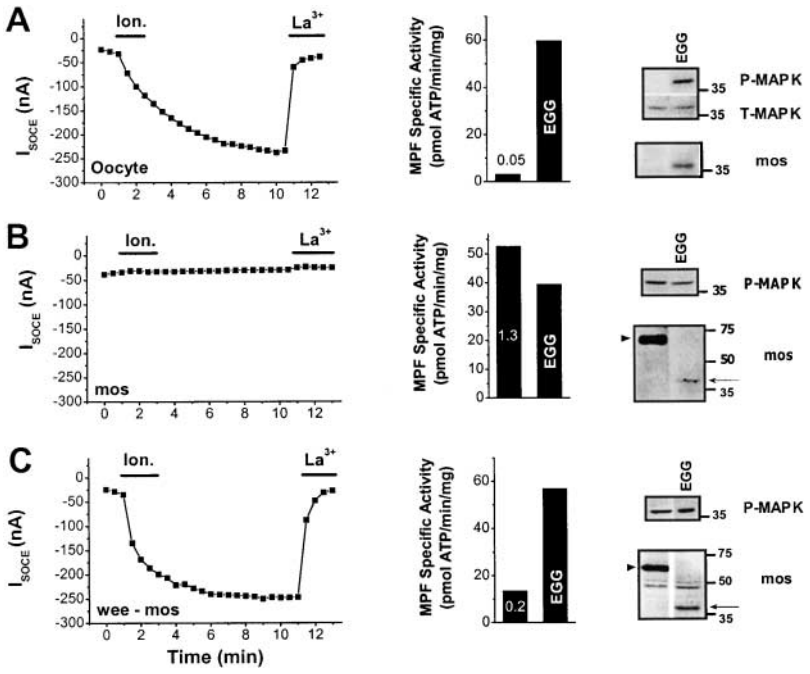

Figure 6. **Representative individual cell data from Wee1- and Mos-injected cells.** MPF, P-MAPK, and Mos Western data are shown in conjunction with the levels of each kinase from a lysate of fully mature eggs (EGG). (A) I_{SOCE} was activated in response to store depletion with ionomycin (10 μM) in an oocyte. MPF, P-MAPK, and Mos were not detected in this cell. (B) A representative cell injected with 10 ng GST–Mos RNA. I_{SOCE} was not activated in response to store depletion. I_{SOCE} was recorded at the $1GVBD_i$ time point in this cell, i.e., at about the same time that GVBD first occurred in the population. MPF and P-MAPK levels were 1.3 and 1.6 times, respectively, higher than those in the egg lysate. GST–Mos protein (arrowhead) levels were 13.1 times higher than egg levels and no endogenous Mos protein (arrow) was detected. (C) A representative cell preinjected with 10 ng GST–107Wee1 RNA 14 h before GST–Mos RNA (10 ng) injection. We recorded I_{SOCE} at the $1GVBD_i$ time point. SOCE was readily activated, in response to store depletion, to levels similar to those found in oocytes. Injection of GST–107Wee1 effectively blocked MPF activation, which was detected at 0.2 times egg level. In contrast, P-MAPK and GST–Mos (arrowhead) were detected at 0.76 and 8.7 times egg levels, respectively.

time course as MPF activation (Fig. 5 C), indicating a strong temporal correlation between MPF levels and I_{SOCE} inactivation. This suggests a role for MPF in I_{SOCE} inactivation. Furthermore, in this case GVBD occurrence also mirrored MPF activation, indicating that MPF effectively targeted its downstream effectors.

If MPF is directly responsible for I_{SOCE} inhibition, then specifically blocking MPF activation should prevent I_{SOCE} inactivation. We accomplished this by injecting a constitutively active Wee1 kinase (GST–107Wee1), which phosphorylates MPF and blocks its activation (Mueller et al., 1995; Howard et al., 1999). Injection of Wee1 did not significantly alter the activation time course of either Mos or MAPK in response to Mos RNA injection (Fig. 5, D and E). However, Wee1 inhibited MPF activation (Fig. 5 F) and prevented GVBD. In these cells with high Mos and MAPK levels and no MPF activity, store depletion activated I_{SOCE} (Fig. 5 F). This shows that MPF activation is necessary for I_{SOCE} inactivation. Note that in Wee1-injected cells, it was possible to record from oocytes for a significantly longer period of time (up to 1.6 $GVBD_i$ or ~10 h) because they did not undergo GVBD. Even at these latter time points (1.3–1.6 $GVBD_i$), I_{SOCE} was clearly detectable in response to store depletion at levels only slightly lower than those in oocytes. Oocytes injected with Wee1 alone (without Mos injection), had I_{SOCE} levels similar to those of control oocytes (1 ± 0.09, $n = 4$), and no detectable MPF or MAPK activation, indicating that Wee1 does not affect I_{SOCE}. Together, these data demonstrate that MPF activation is necessary for I_{SOCE} inactivation.

Examples of single-cell data from Mos- and Wee1/Mos–injected cells are shown in Fig. 6. The oocyte had a robust I_{SOCE} signal and no detectable Mos, MAPK, or MPF (Fig. 6 A). In contrast, a Mos-injected cell showed complete I_{SOCE} inactivation, and high MPF and P-MAPK levels (1.3- and 1.6-fold egg levels, respectively) (Fig. 6 B). Ectopic GST–Mos (Fig. 6 B, arrowhead) was 13.1-fold higher than endogenous Mos levels found in eggs (Fig. 6 B, arrow). No endogenous Mos protein was detected in this cell (Fig. 6 B, arrow). A representative Wee1-preinjected cell (Fig. 6 C) showed levels of ectopic Mos and P-MAPK (8.7- and 0.76-fold egg levels, respectively) similar to a Mos-injected cell. However MPF kinase was not significantly activated (0.2-fold egg level), and I_{SOCE} was readily induced in response to store depletion (Fig. 6 C). This shows that despite the activation of both Mos and P-MAPK for extensive time periods, I_{SOCE} does not inactivate in the absence of MPF activity.

MPF blocks the coupling between store depletion and SOCE activation

We next investigated the mechanism of MPF action in mediating SOCE inactivation. MPF could be either blocking Ca^{2+} influx through SOCE channels, or it could be inhibiting the coupling mechanism between store depletion and SOCE. The molecular identity of the SOCE channel remains unclear, therefore we could not directly test whether MPF phosphorylates SOCE channels. However, by altering the timing of SOCE versus MPF activation, we could determine the target of MPF action. Our rational was to activate I_{SOCE} before MPF levels increased. If MPF phosphorylates SOCE channels and blocks Ca^{2+} influx, then preactivated I_{SOCE} will be inhibited concurrently with MPF activation. Alternatively if MPF blocks the coupling mechanism, then preactivated I_{SOCE} will not be affected by MPF activation.

We activated I_{SOCE} shortly before GVBD in oocytes treated with progesterone, and continuously recorded I_{SOCE} until, and past, GVBD occurrence (Fig. 7 B). GVBD in this cell was apparent ~35 min after store depletion (Fig. 7 B). However, I_{SOCE} remained active with no significant inhibition, even ~20 min after GVBD (Fig. 7 B). We confirmed that GVBD appearance was coupled to the characteristic increase in MPF activity (Fig. 7 B), indicating that

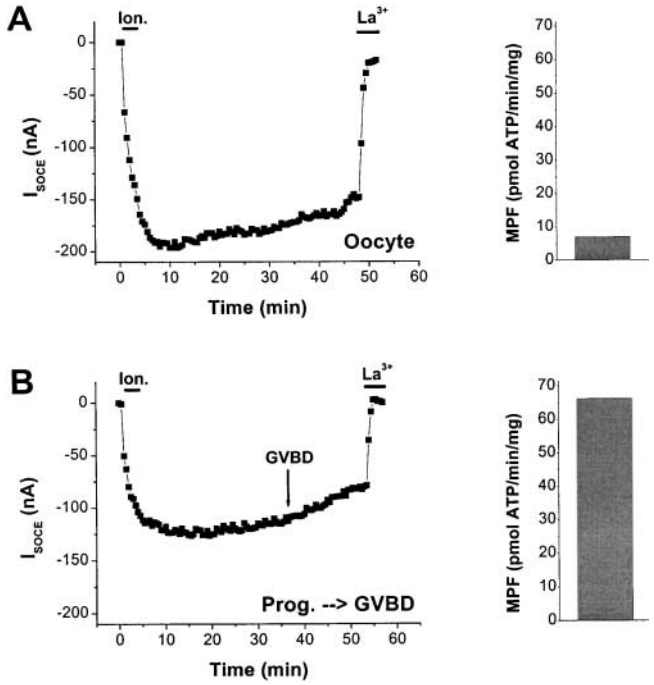

Figure 7. **Continuous recording of I_{SOCE} through the GVBD transition.** (A) Prolonged recording of I_{SOCE} from a control untreated oocyte. MPF activity in this cell is also shown. (B) I_{SOCE} was activated in a progesterone-treated oocyte before GVBD and continuously recorded until, and past, the time point at which GVBD occurred (arrow). At the end of the experiment, the cell was lysed in extraction buffer and MPF activity was measured. This cell had high MPF activity, indicating that the prolonged recording did not interfere with MPF activation at GVBD. MPF activation at GVBD is not able to block I_{SOCE} that has been preactivated before GVBD.

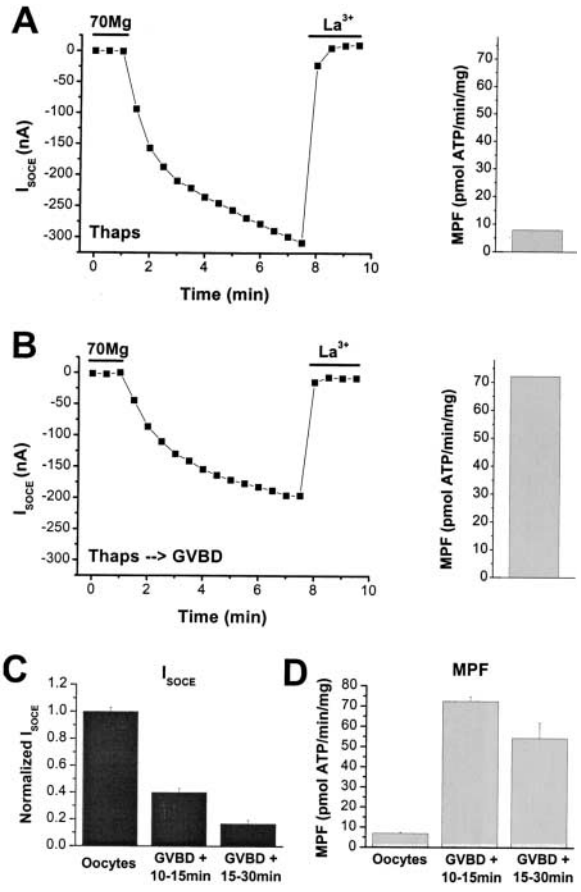

Figure 8. **Pre-activated I_{SOCE} does not inactivate in response to MPF activation.** Oocytes were incubated in Ca^{2+}-free medium (L-15 with Ca^{2+}, buffered at 50 μM), containing thapsigargin (1 μM) to deplete intracellular Ca^{2+} store and activate I_{SOCE}. Cells were voltage clamped in a Ca^{2+}-free solution (70Mg; see Materials and methods) and then switched to a solution containing 30 mM Ca^{2+} (30Ca; see Materials and methods) to induce Ca^{2+} influx through SOCE channels. (A) I_{SOCE} and MPF levels from a control thapsigargin–treated oocyte. (B) Oocytes were treated with progesterone (5 μg/ml) for 1 h and then thapsigargin (1 μM) was added, and the cells were incubated until GVBD occurred. I_{SOCE} was measured ~15 min after GVBD occurrence. I_{SOCE} was still present in this cell, although MPF was activated at high levels, indicating that MPF is unable to block SOCE that has been preactivated before MPF induction. I_{SOCE} (C) and MPF (D) levels in oocytes ($n = 5$) and cells treated with progesterone 10–15 min ($n = 8$) and 15–30 min after GVBD ($n = 7$). I_{SOCE} levels gradually declined after GVBD and MPF levels remained relatively stable.

1,2-bis(2-aminophenoxy) ethane-*N*,*N*,*N*′,*N*′-tetraacetic acid (BAPTA) injection, which was necessary to measure I_{SOCE}, did not interfere with MPF activation. Note that although I_{SOCE} remained activated past GVBD in Fig. 7 B, there was a gradual inhibition in the current over time. Recording I_{SOCE} from a control oocyte for the same prolonged time, shows a similar gradual I_{SOCE} inhibition (Fig. 7 A), indicating that the gradual decline in I_{SOCE} was not due to MPF activation. This shows that once SOCE was activated, increasing MPF levels were not able to inactivate I_{SOCE}. This indicates that MPF does not block Ca^{2+} influx through SOCE channels. However, if MPF is activated before store depletion, SOCE cannot be activated (Fig. 1 F, Fig. 4, B and C, and Fig. 6 B). Therefore, MPF inhibits the coupling mechanism between store depletion and SOCE activation.

A Ca^{2+} signal is required for nuclear envelope breakdown during mitosis (Kao et al., 1990). This does not appear to be the case in *Xenopus* oocytes, because BAPTA injection did not prevent GVBD (Fig. 7 B). However, it is possible that altering Ca^{2+} dynamics by BAPTA injection interferes with the timing of GVBD. This would affect our interpretation of the correlation between GVBD occurrence and I_{SOCE} inhibition. To address this issue, we activated I_{SOCE} before GVBD by depleting Ca^{2+} stores with thapsigargin, independent of BAPTA injection (Fig. 8). Thapsigargin depletes Ca^{2+} stores by blocking the ER Ca^{2+} ATPase, and has been shown to be effective in activating SOCE in *Xenopus* oocytes (Petersen and Berridge, 1994; Machaca and Hartzell, 1999).

As is the case with ionomycin, thapsigargin treatment of eggs after progesterone-induced maturation did not activate I_{SOCE} (4 ± 2.3 nA, $n = 3$). In contrast, thapsigargin activated a robust I_{SOCE} in oocytes (182.7 ± 28 nA, $n = 3$). To test whether preactivated I_{SOCE} is inhibited by MPF activation, we incubated cells in progesterone plus thapsigargin (1 μM), and recorded I_{SOCE} at different time points after GVBD occurrence. I_{SOCE}, preactivated with thapsigargin, was readily apparent 10–15 min after GVBD occurrence

(Fig. 8 B). As expected, this cell contained high levels of MPF activity (Fig. 8 B). A control oocyte, incubated for a similar time in thapsigargin alone, had a large I_{SOCE} and no detectable MPF (Fig. 8 A). These data confirm our conclusion that MPF is unable to inhibit preactivated I_{SOCE}. This indicates that MPF activation at GVBD inhibits coupling of store depletion to SOCE activation.

Interestingly, thapsigargin-induced I_{SOCE} levels were consistently smaller after GVBD as compared with control oocytes (Fig. 8, compare A and B). I_{SOCE} levels measured 10–15 min after GVBD in cells treated with thapsigargin, were at levels 40 ± 3% of control oocyte levels (Fig. 8 C). If I_{SOCE} was recorded 15–30 min after GVBD occurred, I_{SOCE} levels declined further, to 17 ± 3% of oocyte levels (Fig. 8 C). Therefore, preactivated I_{SOCE} decreases gradually after GVBD.

What is the reason for this gradual downregulation of I_{SOCE} after GVBD? In oocytes and other cell types, Ca^{2+} store depletion results in the activation of SOCE. Therefore, a positive signal (i.e., the coupling species) is induced resulting in SOCE activation. Once the Ca^{2+} store is refilled, SOCE is downregulated. This argues for the presence of a constitutive mechanism that downregulates I_{SOCE} in the absence of the coupling species. As shown above, MPF activation blocks coupling between store depletion and SOCE activation. This would eliminate the positive signal to maintain active SOCE and would lead to SOCE downregulation. Therefore, the gradual inhibition of preactivated I_{SOCE} after GVBD is likely due to the block of Ca^{2+} store–SOCE coupling by MPF and constitutive downregulation of SOCE.

Discussion

MPF is required for SOCE inactivation

Oocyte maturation entails a complex series of biochemical and morphological adaptations that transform immature oocytes into fertilization-competent eggs, able to support embryonic development. Early electron microscopy studies have described morphological changes that occur concomitant with *Xenopus* oocyte maturation (for review see Bement and Capco, 1990). Furthermore, extensive studies have characterized biochemical cascades that drive oocyte maturation (Nebreda and Ferby, 2000). There remains much to be learned about how these signal transduction cascades regulate physiologically relevant pathways during oocyte maturation. Here we describe the relationship between the Mos–MAPK–MPF kinase cascade and SOCE. Differentiation of Ca^{2+} signaling pathways during oocyte maturation is a prerequisite for proper egg activation after fertilization. This is because the Ca^{2+} wave at fertilization mediates egg activation by inducing the block to polyspermy and releasing the MII block (Bement and Capco, 1990). SOCE inactivates specifically at the GVBD stage of *Xenopus* oocyte maturation (Fig. 1 F) (Machaca and Haun, 2000). This inactivation is likely to be important physiologically because *Xenopus* eggs can be artificially activated by pricking with a glass needle, but only in the presence of extracellular Ca^{2+} (Wolf, 1974). Therefore, Ca^{2+} entry is sufficient to stimulate egg activation, probably due to changes in the sensitivity and organization of the Ca^{2+} release machinery. Consequently, inactivation of I_{SOCE} at the GVBD stage, soon after entry into meiosis, may function as a safety measure to prevent premature egg activation before fertilization.

Inactivation of ionic currents during M phase is not a peculiar property of I_{SOCE} in *Xenopus* oocytes, and has been described for other membrane proteins and cell types. For example, in *Xenopus* oocytes, amino acid and phosphate transporters are downregulated, but not completely inactivated, during oocyte maturation (Richter et al., 1984). In the same respect, surface levels of the Na^+–K^+–ATPase (Schmalzing et al., 1990) and of β1 integrin (Muller et al., 1993) decrease during *Xenopus* oocyte maturation. Recently, several exogenously expressed channels have been shown to be downregulated during oocyte maturation (Shcherbatko et al., 2001). We have obtained similar results with exogenously expressed glutamate receptor (GluR3; unpublished data). In contrast, the levels of Ca^{2+}-activated Cl^- current ($I_{Cl,Ca}$) do not decrease during maturation (Machaca and Haun, 2000). Therefore, there is extensive, specific regulation of membrane proteins during *Xenopus* oocyte maturation. Regulation of membrane proteins during M phase is not limited to *Xenopus* oocytes. SOCE has been shown to inactivate during mitosis of HeLa cells (Preston et al., 1991), and membrane trafficking in general is inhibited during mammalian cell mitosis (Warren, 1993). Therefore, determining the molecular mechanisms controlling SOCE inactivation during *Xenopus* oocyte maturation provides valuable insights into the regulation of plasma membrane protein levels during M phase.

Our results argue that activation of MPF leads to uncoupling of store depletion from SOCE. Several lines of evidence support this conclusion. During progesterone-induced maturation, I_{SOCE} inactivation at GVBD coincides with MPF activation (Figs. 1 and 2). Furthermore, regardless of the method by which we induced oocyte maturation (progesterone, cyclin B1, or Mos injection), every cell in which I_{SOCE} was inactivated had high MPF activity. In addition, cells with low MPF activity always activated I_{SOCE} in response to store depletion (Figs. 3–6). Out of 155 individual cells from which we recorded I_{SOCE} and measured kinase activity, not a single cell deviated from these criteria. Finally, Mos injection did not lead to SOCE inactivation when MPF was inhibited (Fig. 5 F). Mos injection activates the MAPK cascade (Fig. 5 B), and leads to the activation of other signal transduction cascades important for oocyte maturation. Specifically blocking MPF activation under these conditions with Wee1, reversed I_{SOCE} inactivation. This demonstrates that MPF activation during oocyte maturation is necessary for I_{SOCE} inactivation.

Is MPF activation sufficient for I_{SOCE} inactivation? Progesterone (Figs. 1 and 2) and Mos RNA injection data (Fig. 5 C) argue that it is. Under these conditions, the time course of MPF activation paralleled that of I_{SOCE} inhibition. In contrast, rapid activation of MPF with cyclin B1 injection revealed a delay before GVBD and SOCE inactivation (Fig. 3 A). As discussed above this time lag could be an artifact of ectopic MPF activation, and not a true reflection of endogenous MPF activity. Two pools of $p34^{cdc2}$ kinase exist in the immature *Xenopus* oocyte, an inactive preMPF pool and a 10-fold excess-free $p34^{cdc2}$ protein pool (Kobayashi et al., 1991). Progesterone and cyclin B1 likely activate the two $p34^{cdc2}$ pools

differentially, which would explain the delay in GVBD after cyclin B1 injection. Nonetheless, after progesterone, Mos, or cyclin B1 injection, I_{SOCE} inactivation correlates temporally with GVBD. As GVBD is a target for MPF, we argue that MPF activation is sufficient for I_{SOCE} inactivation.

In contrast to the MPF requirement for SOCE inactivation, we did not observe any correlation between I_{SOCE} levels and P-MAPK and Mos levels (Figs. 3–6). This indicates that neither Mos kinase nor the MAPK cascade plays a direct role in I_{SOCE} inactivation.

MPF blocks coupling of store depletion to SOCE activation

Activation of MPF before Ca^{2+} store depletion blocks SOCE activation. This was true whether MPF was activated by progesterone treatment (Figs. 1 and 2), Mos RNA injection (Figs. 5 and 6), or cyclin B1 protein injection (Figs. 3 and 4). In contrast, when MPF was induced after SOCE activation, it was unable to block I_{SOCE} (Figs. 7 and 8). This indicates that MPF blocks SOCE activation and not the current through SOCE channels. MPF could uncouple store depletion from SOCE activation by inhibiting the coupling species. Alternatively, MPF could target SOCE channels and prevent them from responding to the coupling species, without inhibiting the coupling species. In either case, our results demonstrate that MPF blocks coupling of Ca^{2+} store depletion to SOCE activation. Further investigations of the downstream targets of MPF will provide critical insights into the identity of the elusive coupling mechanism between store depletion and SOCE activation.

MPF is a member of the cyclin-dependent kinase family or cell cycle regulators. Cyclin-dependent kinases are master regulators of entry and progression through both mitosis and meiosis (Morgan, 1997). In that capacity, MPF controls various cellular processes crucial for meiotic progression. For example, MPF induces GVBD and stabilizes Mos kinase, which is a component of CSF (Palmer and Nebreda, 2000). CSF is required to maintain metaphase II arrest until fertilization (Masui, 1991). Our results indicate that SOCE inactivation can now be added to the list of cellular processes driven by MPF. Interestingly, MPF has recently been shown to regulate Ca^{2+} oscillations at fertilization in ascidian eggs (Levasseur and McDougall, 2000). The differentiation of Ca^{2+} signaling pathways is an important element of oocyte maturation. The fact that MPF regulates both Ca^{2+} release and Ca^{2+} influx in oocytes from different species strongly supports the idea that Ca^{2+} signaling is tightly controlled and functionally relevant during meiosis.

Materials and methods

Oocyte isolation and enucleation

X. laevis females (*Xenopus* Express) were anesthetized by immersion in Tricaine (1 g/liter, pH 7) for 5–10 min. Ovarian follicles were removed and digested in Ca^{2+}-free Ringer's solution (96 mM NaCl, 2 mM KCl, 5 mM $MgCl_2$, 5 mM Hepes, pH 7.6), containing 2 mg/ml collagenase type IA (Sigma-Aldrich) for 2 h at room temperature. The oocytes were extensively rinsed with Ringer's solution and incubated in 0.5× L-15 medium (GIBCO BRL) at 18°C. Oocytes were used for up to 4 d after isolation. Oocyte maturation was induced by incubating cells in L-15 containing 5 μg/ml progesterone. In some experiments oocytes were enucleated. This was accomplished by poking a hole on the animal pole using a glass needle, followed by the application of gentle pressure on the oocyte. This results in the expulsion of the germinal vesicle (nucleus). Oocytes were allowed to recover for at least 30 min before electrophysiological recordings.

Electrophysiological methods

The I_{SOCE} was measured as previously described (Machaca and Haun, 2000). In brief, SOCE was activated by depletion of intracellular Ca^{2+} stores with either ionomycin (10 μM) or thapsigargin (1 μM for ≥3 h). Oocytes were injected with 7 nmoles BAPTA before store depletion, to buffer intracellular Ca^{2+} rise and block the endogenous Ca^{2+}-activated Cl^- current ($I_{Cl,Ca}$), which would otherwise mask the I_{SOCE}. Assuming an oocyte volume of 1 μl, this would result in a final concentration of ~7 mM BAPTA, which completely blocks $I_{Cl,Ca}$. I_{SOCE} was typically measured at the hyperpolarizing potential of −140 mV. This is because we wanted to maximize I_{SOCE}, to most accurately determine the level of inactivation. *Xenopus* oocytes or eggs were voltage clamped with two microelectrodes by the use of a GeneClamp 500 (Axon Instruments, Inc.). Electrodes were filled with 3 M KCl and had resistances of 0.5–2 MΩ. Voltage stimulation and data acquisition were controlled using Curcap30 (Bill Goolsby, Emory University, Atlanta, GA). Current data was filtered at 10 kHz, digitized, and analyzed using Origin® software (Microcal Software, Inc.). Some experiments used 30Ca or 70Mg solutions (30Ca: 55 mM NaCl, 30 mM $CaCl_2$, 10 mM Hepes, pH 7.4; 70Mg: 70 mM $MgCl_2$, 10 mM Hepes, pH 7.4).

MPF kinase assay

MPF kinase activity was measured by lysing an oocyte in 50 μl extraction buffer (80 mM β-glycerophosphate, 20 mM Hepes, pH 7.5, 20 mM EGTA, 15 mM $MgCl_2$, 1 mM sodium vanadate, 50 mM NaF, 1 mM DTT, 10 μg/ml aprotinin, 50 μg/ml leupeptin, 1 mM PMSF). Lysates were centrifuged at 16,000 *g* for 5 min, and the supernatant was stored at −70°C. MPF activity was measured using the SignaTECT™ cdc2 kinase assay system (Promega), according to manufacturer's recommendations. This assay measures MPF activity in terms of the phosphorylation of a specific substrate, i.e., a biotinylated peptide derived from histone H1 (PKTPKKAKKL).

Western blotting

P-MAPK, total MAPK, and Mos protein levels were measured by Western blotting. Lysates were prepared as for the MPF assay, and protein concentration was measured using the Bradford assay (Bio-Rad Laboratories). SDS-PAGE gels were loaded with equal amounts of protein, transferred onto Immobilon P-PVDF membranes (Millipore), and probed with the appropriate primary antibody: anti–phospho-MAPK and anti–total MAPK (Cell Signaling Technology) or anti-Mos antibodies (Santa Cruz Biotechnology, Inc.). This was followed by the appropriate HRP-conjugated secondary antibody (Jackson ImmunoResearch Laboratories) and detected using the ECL Plus Western blot detection system (Amersham Pharmacia Biotech). Westerns were visualized using a STORM™ system (Molecular Dynamics), which allowed a linear response to be measured from the band intensity on the Western blot. This was crucial for accurate quantification of P-MAPK and Mos protein levels. To control for variability between different trials, a large batch of lysate from mature eggs was prepared for both P-MAPK and Mos. This control lysate was loaded on each gel used for quantifying P-MAPK and Mos levels. The same lysate was used for all P-MAPK and Mos gels, respectively, which provided a consistent internal control for all the experiments. Using this method we could faithfully reproduce (with <15% error margin) P-MAPK and Mos protein levels from the same sample in different experiments.

Reagents

The following reagents were used: ionomycin and PD98059 (Calbiochem); thapsigargin (Molecular Probes Inc.); progesterone, salts, and other reagents (Sigma-Aldrich). The following constructs were provided by A.M. MacNicol (University of Arkansas Medical Science): GST–Mos; GST–107Wee1, which encodes a constitutively active Wee1 kinase (Mueller et al., 1995; Howard et al., 1999); and a His_6-tagged Δ87cyclin B1 protein (Kumagai and Dunphy, 1995; Howard et al., 1999). Oocytes were injected with 10 ng of the GST–Mos and GST–107Wee1 RNAs and ~200 pg Δ87cyclin B1 protein.

We are grateful to Angus MacNicol for various clones and helpful discussion. We would like to thank David Clapham, Angus MacNicol, and Larry Suva for comments on the manuscript.

This work was supported by a grant from the National Institutes of Health (GM-61829).

Submitted: 11 October 2001
Revised: 15 November 2001
Accepted: 19 November 2001

References

Bement, W.M., and D.G. Capco. 1990. Transformation of the amphibian oocyte into the egg: structural and biochemical events. *J. Electron Microsc. Tech.* 16: 202–234.

Berridge, M.J. 1995. Capacitative calcium entry. *Biochem. J.* 312:1–11.

Colman, A., E.A. Jones, and J. Heasman. 1985. Meiotic maturation in Xenopus oocytes: a link between the cessation of protein secretion and the polarized disappearance of Golgi apparati. *J. Cell Biol.* 101:313–318.

Cross, N.L. 1981. Initiation of the activation potential by an increase in intracellular calcium in eggs of the frog, *Rana pipiens*. *Dev. Biol.* 85:380–384.

Csutora, P., Z. Su, H.Y. Kim, A. Bugrim, K.W. Cunningham, R. Nuccitelli, J.E. Keizer, M.R. Hanley, J.E. Blalock, and R.B. Marchase. 1999. Calcium influx factor is synthesized by yeast and mammalian cells depleted of organellar calcium stores. *Proc. Natl. Acad. Sci. USA.* 96:121–126.

Dolmetsch, R.E., and R.S. Lewis. 1994. Signaling between intracellular Ca^{2+} stores and depletion-activated Ca^{2+} channels generates $[Ca^{2+}]_i$ oscillations in T lymphocytes. *J. Gen. Physiol.* 103:365–388.

Fanger, C., M. Hoth, G.R. Crabtree, and R.S. Lewis. 1995. Characterization of T cell mutants with defects in capacitative calcium entry: genetic evidence for the physiological roles of CRAC channels. *J. Cell Biol.* 131:655–667.

Fomina, A.F., and M.C. Nowycky. 1999. A current activated on depletion of intracellular Ca^{2+} stores can regulate exocytosis in adrenal chromaffin cells. *J. Neurosci.* 19:3711–3722.

Freeman, R.S., S.M. Ballantyne, and D.J. Donoghue. 1991. Meiotic induction by Xenopus cyclin B is accelerated by coexpression with mosXe. *Mol. Cell Biol.* 11:1713–1717.

Girard, S., and D.E. Clapham. 1993. Acceleration of intracellular calcium waves in *Xenopus* oocytes by calcium influx. *Science.* 260:229–232.

Grey, R.D., P.K. Working, and J.L. Hedrick. 1976. Evidence that the fertilization envelope blocks sperm entry in eggs of *Xenopus laevis*: interaction of sperm with isolated envelopes. *Dev. Biol.* 54:52–60.

Homa, S.T., J. Carroll, and K. Swann. 1993. The role of calcium in mammalian oocyte maturation and egg activation. *Human Reproduction.* 8:1274–1281.

Howard, E.L., A. Charlesworth, J. Welk, and A.M. MacNicol. 1999. The mitogen-activated protein kinase signaling pathway stimulates mos mRNA cytoplasmic polyadenylation during *Xenopus* oocyte maturation. *Mol. Cell. Biol.* 19:1990–1999.

Kao, J.P., J.M. Alderton, R.Y. Tsien, and R.A. Steinhardt. 1990. Active involvement of Ca^{2+} in mitotic progression of Swiss 3T3 fibroblasts. *J. Cell Biol.* 111:183–196.

Kiselyov, K., X. Xu, G. Mozhayeva, T.H. Kuo, I.N. Pessah, G. Mignery, X. Zhu, L. Birnbaumer, and S. Muallem. 1998. Functional interaction between $InsP_3$ receptors and store-operated Htrp3 channels. *Nature.* 396:478–482.

Kline, D., and R. Nuccitelli. 1985. The wave of activation current in the *Xenopus* egg. *Dev. Biol.* 111:471–487.

Kobayashi, H., J. Minshull, C. Ford, R. Golsteyn, R. Poon, and T. Hunt. 1991. On the synthesis and destruction of A- and B-type cyclins during oogenesis and meiotic maturation in *Xenopus laevis*. *J. Cell Biol.* 114:755–765.

Koizumi, S., and K. Inoue. 1998. Functional coupling of secretion and capacitative calcium entry in PC12 cells. *Biochem. Biophys. Res. Commun.* 247:293–298.

Kumagai, A., and W.G. Dunphy. 1995. Control of the Cdc2/cyclin B complex in *Xenopus* egg extracts arrested at a G2/M checkpoint with DNA synthesis inhibitors. *Mol. Biol. Cell.* 6:199–213.

Levasseur, M., and A. McDougall. 2000. Sperm-induced calcium oscillations at fertilization in ascidians are controlled by cyclin B1-dependent kinase activity. *Development.* 127:631–641.

Machaca, K., and H.C. Hartzell. 1999. Reversible Ca gradients between the subplasmalemma and cytosol differentially activate Ca-dependent Cl currents. *J. Gen. Physiol.* 113:249–266.

Machaca, K., and S. Haun. 2000. Store-operated calcium entry inactivates at the germinal vesicle breakdown stage of *Xenopus* meiosis. *J. Biol. Chem.* 275: 38710–38715.

Machaca, K., Z. Qu, A. Kuruma, H.C. Hartzell, and N. McCarty. 2001. The endogenous calcium-activated Cl channel in *Xenopus* oocytes: a physiologically and biophysically rich model system. *In* Calcium Activates Chloride Channels. Current Topics in Membranes. C.M. Fuller, editor. Academic Press, San Diego.

Masui, Y. 1991. The role of cytostatic factor (CSF) in the control of oocyte cell cycles. *Dev. Growth Differ.* 33:543–551.

Masui, Y., and H.J. Clarke. 1979. Oocyte maturation. *Int. Rev. Cytol.* 57:185–282.

Meyerhof, P.G., and Y. Masui. 1979. Properties of a cytostatic factor from *Xenopus laevis* eggs. *Dev. Biol.* 72:182–187.

Morgan, D.O. 1997. Cyclin-dependent kinases: engines, clocks, and microprocessors. *Annu. Rev. Cell Dev. Biol.* 13:261–291.

Mueller, P.R., T.R. Coleman, and W.G. Dunphy. 1995. Cell cycle regulation of a *Xenopus* Wee1-like kinase. *Mol. Biol. Cell.* 6:119–134.

Muller, A.H., V. Gawantka, X. Ding, and P. Hausen. 1993. Maturation induced internalization of beta 1-integrin by *Xenopus* oocytes and formation of the maternal integrin pool. *Mech. Dev.* 42:77–88.

Nebreda, A.R., and I. Ferby. 2000. Regulation of the meiotic cell cycle in oocytes. *Curr. Opin. Cell Biol.* 12:666–675.

Palmer, A., and A.R. Nebreda. 2000. The activation of MAP kinase and p34cdc2/cyclin B during the meiotic maturation of *Xenopus* oocytes. *Prog. Cell Cycle Res.* 4:131–143.

Parekh, A.B., and R. Penner. 1997. Store depletion and calcium influx. *Physiological Reviews.* 77:901–930.

Petersen, C.C., and M.J. Berridge. 1994. The regulation of capacitative calcium entry by calcium and protein kinase C in *Xenopus* oocytes. *J. Biol. Chem.* 269:32246–32253.

Preston, S.F., R.I. Sha'afi, and R.D. Berlin. 1991. Regulation of Ca^{2+} influx during mitosis: Ca^{2+} influx and depletion of intracellular Ca^{2+} stores are coupled in interphase but not mitosis. *Cell Regulation*. 2:915–925.

Qian, Y.W., E. Erikson, and J.L. Maller. 1999. Mitotic effects of a constitutively active mutant of the *Xenopus* polo-like kinase Plx1. *Mol. Cell Biol.* 19:8625–8632.

Qian, Y.W., E. Erikson, F.E. Taieb, and J.L. Maller. 2001. The polo-like kinase Plx1 is required for activation of the phosphatase Cdc25C and cyclin B-Cdc2 in *Xenopus* oocytes. *Mol. Biol. Cell.* 12:1791–1799.

Randriamampita, C., and R.Y. Tsien. 1993. Emptying of intracellular calcium stores release a novel small messenger that stimulates calcium influx. *Nature.* 364:809–814.

Richter, H.P., D. Jung, and H. Passow. 1984. Regulatory changes of membrane transport and ouabain binding during progesterone-induced maturation of *Xenopus* oocytes. *J. Membr. Biol.* 79:203–210.

Sagata, N. 1997. What does Mos do in oocytes and somatic cells? *BioEssays.* 19:13–21.

Schmalzing, G., P. Eckard, S. Kroner, and H. Passow. 1990. Downregulation of surface sodium pumps by endocytosis during meiotic maturation of *Xenopus laevis* oocytes. *Am. J. Physiol.* 258:C179–C184.

Serafini, A., R.S. Lewis, N.A. Clipstone, R. Bram, C. Fanger, S. Fiering, L.A. Herzenberg, and G.R. Crabtree. 1995. Isolation of mutant T lymphocytes with defects in capacitative calcium entry. *Immunity.* 3:239–250.

Shcherbatko, A.D., C.M. Davenport, J.C. Speh, S.R. Levinson, G. Mandel, and P. Brehm. 2001. Progesterone treatment abolishes exogenously expressed ionic currents in *Xenopus* oocytes. *Am. J. Physiol.* 280:C677–C688.

Smith, L.D. 1989. The induction of oocyte maturation: transmembrane signaling events and regulation of the cell cycle. *Development.* 107:685–699.

Somasundaram, B., J.C. Norman, and M.P. Mahaut-Smith. 1995. Primaquine, an inhibitor of vesicular transport, blocks the calcium-release-activated current in rat megakaryocytes. *Biochem. J.* 309:725–729.

Stricker, S.A. 2000. Comparative biology of calcium signaling during fertilization and egg activation in animals. *Dev. Biol.* 211:157–176.

Warren, G. 1993. Membrane partitioning during cell division. *Annu. Rev. Biochem.* 62:323–348.

Wolf, D.P. 1974. The cortical granule reaction in living eggs of the toad, *Xenopus laevis*. *Dev. Biol.* 36:62–71.

Yamashita, M., K. Mita, N. Yoshida, and T. Kondo. 2000. Molecular mechanisms of initiation of oocyte maturation: general and species-specific aspects. *Prog. Cell Cycle Res.* 4:115–129.

Yao, Y., A.V. Ferrer-Montiel, M. Montal, and R.Y. Tsien. 1999. Activation of store-operated Ca^{2+} current in *Xenopus* oocytes requires SNAP-25 but not a diffusible messenger. *Cell.* 98:475–485.